Deep-Sea Research II 123 (2016) 135–144

Contents lists available at ScienceDirect

Deep-Sea Research II

journal homepage: www.elsevier.com/locate/dsr2

Sedimentation of particulate organic carbon on the Amundsen Shelf, Antarctica

Minkyoung Kim [a], Jeomshik Hwang [a,b,*], Sang H. Lee [c], Hyung J. Kim [d], Dongseon Kim [d], Eun J. Yang [e], SangHoon Lee [e]

[a] Earth and Environmental Sciences, Seoul National University, Seoul 151-742, South Korea
[b] Research Institute of Oceanography (RIO), Seoul National University, Seoul, South Korea
[c] Pusan National University, Busan, South Korea
[d] Korea Institute of Ocean Science & Technology, Ansan, South Korea
[e] Korea Polar Research Institute, Incheon, South Korea

ARTICLE INFO

Available online 8 August 2015

Keywords:
Amundsen Shelf
Polynya
Sedimentary organic carbon
Organic carbon sequestration
Radiocarbon
Global carbon cycling

ABSTRACT

We examined the recent history of sedimentary organic carbon (SOC) accumulation on the western Amundsen Shelf, to help characterize the biological carbon pump in the Amundsen Sea, Antarctica. Vertical sedimentary profiles (in the upper 21-cm) of SOC content, radio- and stable-carbon isotopes were obtained at four locations in the western Amundsen Sea: near the shelf break, inside the polynya near the Dotson Ice Shelf, and at both the periphery and the center of the Amundsen Sea polynya. Profiles were representative not only of various distances from the coast, but also of various summertime sea ice conditions and bottom depths. The SOC content (up to 1.1%) and the radiocarbon content were distinctly higher at the periphery and at the center of the polynya than at the other sites. The SOC and ^{14}C contents were generally consistent with the spatial distribution of primary productivity in the surface water. A linear SOC accumulation rate of about 1.0 g C m^{-2} yr^{-1} was determined from the conventional ^{14}C ages of bulk SOC below the surface mixed layer at the periphery and at the center of the polynya, for the time period of 3.1–4.7 kyr before present (BP). This linear SOC accumulation rate was about 20 times greater than the rates determined at the two other sites for the period of 4.6–15.7 kyr BP. Note that all values are for uncorrected ^{14}C ages. At the center of the polynya, a sudden change in SOC accumulation rate was observed at about 16 cm depth, corresponding to 4.7 kyr BP, implying that changes (during this time period) in physical environments greatly affected primary production, SOC burial and/or supply of allochthonous particles to this site. The vertical distribution of ^{14}C content in the sediments implies that aged organic matter, likely associated with resuspended sediments, was also being deposited inside the polynya, in addition to autochthonous biogenic particles. If our estimation of SOC accumulation is extrapolated to the western Amundsen Shelf between 110°W and 120°W, approximately 3×10^{10} g C yr^{-1} is buried on the shelf, with ~90% of SOC accumulation occurring in the Amundsen Sea polynya.

1. Introduction

The Amundsen Sea, located between the Ross Sea and the Bellingshausen Sea in the western Antarctic (Fig. 1), is rapidly responding to global climate change. Ice shelves and glaciers in the Amundsen Sea have been shrinking at a remarkable rate (Rignot et al., 2008). Sea ice coverage is decreasing especially fast in the western Antarctic (Stammerjohn et al., 2012).

Polynyas, seasonally open water surrounded by sea ice in high latitude regions, often exhibit high primary productivity (Zielinski and Gersonde, 1997; Becquevort and Smith Jr., 2001; Arrigo and van Dijken, 2003). Among the Antarctic polynyas, two coastal polynyas in the Amundsen Sea (the Amundsen Sea polynya and the Pine Island Bay polynya) are reportedly the most productive regions, with satellite-based annual primary production reaching up to 160 g C m^{-2} yr^{-1} (Arrigo and van Dijken, 2003; Arrigo et al., 2012; Fragoso and Smith Jr., 2012). As the ice shelf (Rignot et al., 2008; Pritchard et al., 2009) and sea ice cover (Walker et al., 2007; Stammerjohn et al., 2012) shrink,

* Corresponding author at: Earth and Environmental Sciences, Seoul National University, Seoul 151-742, South Korea. Tel.: +82 2 880 6751.
E-mail address: jeomshik@snu.ac.kr (J. Hwang).

http://dx.doi.org/10.1016/j.dsr2.2015.07.018
0967-0645/

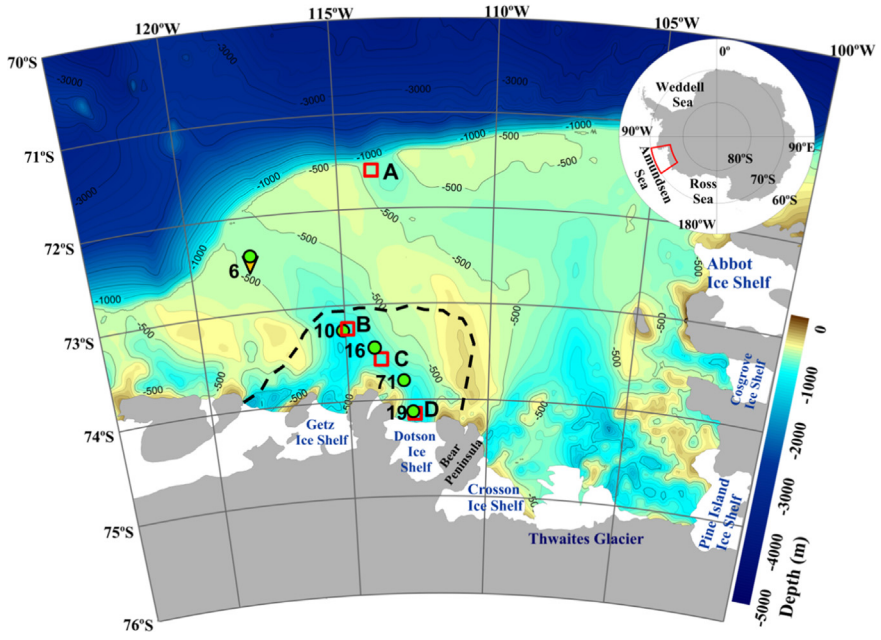

Fig. 1. Bathymetry and sampling locations of sediments (squares) and suspended particles in surface waters (circles). The numbers by the circles are the station numbers. The reversed triangle indicates the location of the sediment trap. The dashed line indicates 10% sea ice concentration in February 2012, as the boundary of the Amundsen Sea Polynya.

more extensive areas of the Amundsen Sea may start resembling polynya in the near future.

Primary production and subsequent export of particulate organic carbon (POC) in the form of sinking particles is an essential part of the biological pump (Volk and Hoffert, 1985). The role of the polynyas in CO_2 absorption and their consequent impact on global carbon cycling is affected by the efficiency of the biological pump. However, our understanding of the behavior of POC after its production in the Amundsen Sea is greatly limited. Recently, Ducklow et al. (2015) reported sinking particle flux obtained from a sediment trap that was moored for a year at the center of the Amundsen Sea polynya. A brief but high particle flux event in the austral summer (up to 96 mg C m^{-2} d^{-1}) reflected an intensive plankton bloom in the surface water of the polynya (Ducklow et al., 2015). During the same time period, a comparable POC flux (up to 55 mg C m^{-2} d^{-1}) was also observed in the sea ice zone of the Amundsen Sea (Kim et al., 2015). However, the fate of this exported POC on the Amundsen Shelf is not well studied.

A close examination of the past record of sedimentary organic carbon (SOC) accumulation may allow us to better predict the future behavior of carbon sequestration in this region. Studies of SOC accumulation rate and radiocarbon chronology on the Amundsen Shelf have mainly focused on deglaciation history, i.e., $>10{,}000$ yr (e.g., Smith et al., 2011). We examined the nature of SOC accumulation on the Amundsen Shelf as part of a larger study to characterize the current status of the biological pump and its operation in the recent past (up to several thousand years ago). We studied the biogeochemical properties of sedimentary organic matter at four locations with different physical characteristics (such as summertime sea ice concentration and bottom depth) on the western Amundsen Shelf and attempted to reconstruct the past depositional environment, mainly based on radiocarbon analysis of bulk SOC in the upper 21-cm sediment horizons.

2. Sample collection and analyses

2.1. Sample collection

Suspended particle and sediment samples were collected during a cruise aboard the IBRV *Araon* from January to March 2012 (Fig. 1). Sediment samples were collected at three locations along the western paleo ice stream trough from the Dotson Ice Shelf (Dotson trough) and one location near the shelf break in the western Amundsen Sea (Fig. 1). Station A (71.70°S, 114.04°W; 543 m bottom depth) is located in the sea ice zone near the shelf break of the Amundsen Sea. Unfavorable sea ice conditions and coarse sediment composition (suggested by a multi-beam survey) discouraged us from collecting sediments near the shelf break inside the Dotson trough. Station B (73.23°S, 114.91°W; 802 m) is located at the periphery of the Amundsen Sea polynya. Even during the summer minimum in sea ice concentration, Station B was not fully rid of sea ice unlike the central polynya (Fig. 2). We used a multi-core (KC Denmark A/S) at Station B. Station C (73.62°S, 113.80°W; 777 m) represents the central polynya where the sea ice concentration was reduced to near zero in the austral summer (Fig. 2). Station D (74.20°S, 112.52°W; 1080 m) is within the Amundsen Sea polynya but is characterized by close proximity to the Dotson Ice Shelf (approximately 2 km away from the ice shelf). After several failures with the multi-core, a box-core (Marine Tech. Korea) was used at Stations A, C, and D. Upon detachment of the box-core canister, plastic barrels of 8 cm diameter and 60 cm length were gently pushed in for sub-cores. Each sediment core was sliced into 1-cm layers on board and stored in pre-baked (450 °C for 4 h) glass jars and kept frozen until analysis.

Suspended particles in the surface water were collected by filtering sea water drained from the ship's uncontaminated sea-water intake system (~7 m below the surface) on pre-baked (450 °C for 4 h) 47 mm GF/F filters (0.7 μm nominal pore size, Whatman) under low vacuum (500 mmHg) without any pre-filtration at five sites on the shelf (Fig. 1). These suspended particle samples contained plankton in addition to phytodetritus. Each filter was folded and stored frozen (−20 °C) in a pre-combusted aluminum foil pouch until further analysis.

2.2. Sample analyses

In the laboratory, the frozen sediment samples were thawed and dried in an oven at 45 °C prior to analyses. For carbon concentration and isotope analyses, each sediment sample was finely ground, weighed in a silver cup, and fumigated with concentrated HCl in a desiccator for 20 h at room temperature (Hedges and Stern, 1984; Komada et al., 2008). The samples then placed on a heating plate at about 45 °C for 4 h to remove HCl vapor. The sample in a silver cup was

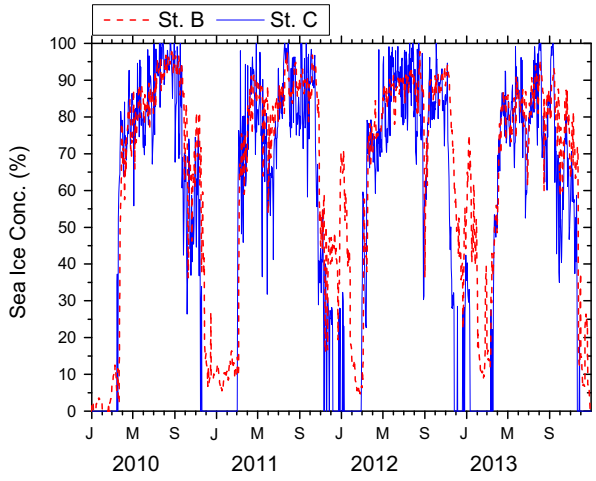

Fig. 2. Temporal variation of sea ice concentration at Stations B (dashed line) and C (solid line) from January 2010 to December 2013 (data from the European Centre for Medium-Range Weather Forecasts, ECMWF).

transferred into a quartz tube with CuO. The quartz tube was evacuated on a vacuum line, flame-sealed, and combusted at 850 °C for 4 h. The resultant CO_2 gas was cryogenically purified and collected in a specific part of the vacuum line, the volume of which was known. The amount of CO_2 gas was measured using the registered pressure. The uncertainty for this manometric determination of CO_2 gas is ± 3% relative standard deviation (RSD), obtained by repetitive processing of glucose. These CO_2 samples were stored in Pyrex tubes and analyzed for carbon isotopes at the National Ocean Sciences Accelerator Mass Spectrometry Facility at the Woods Hole Oceanographic Institution (NOSAMS WHOI) following standard techniques (McNichol et al., 1994). Radiocarbon results are reported in $\Delta^{14}C$, the per mil deviation of the $^{14}C/^{12}C$ ratio relative to the oxalic acid standard (OX-I), corrected to $\delta^{13}C$ of −25‰ (relative to PDB standard) to remove any isotopic fractionation effect (Broecker and Olson, 1959; Stuiver and Polach, 1977). Uncertainties for $\Delta^{14}C$ and $\delta^{13}C$ determined by multiple duplicate-analyses in our laboratory were less than 10‰ and 0.1‰, respectively. The $\Delta^{14}C$ values of two separate runs of OX-I standard processed in the same way were 36‰ and 46‰, demonstrating that our carbon isotope results were within the uncertainty range.

Core-top samples (0–1 cm) at all stations and selected layers at Station C were analyzed for total carbon (TC) and total nitrogen (TN) with an elemental analyzer (Flash 1112, CE Instrument) at the Korea Basic Science Institute. TC and TN measurements had an uncertainty of 0.9 and 1.7% RSD, respectively (based on 5 duplicate samples). At Stations A, B, and D, a subset of samples were analyzed for TC, total inorganic carbon (TIC), and TN at the Korea Institute of Ocean Science and Technology (KIOST). TC and TN were measured for ~15 mg samples with an elemental analyzer (Flash 2000, Thermo). Based on repeated analyses of an L-Cystine standard, the uncertainty was 1.3% RSD for TC measurements and 1.2% RSD for TN measurements. TIC content was determined by coulometric titration (CM240, UIC) of ~15 mg samples. An RSD of 0.7% was obtained based on repeated analyses of a $CaCO_3$ standard. Organic carbon content, calculated as the difference between TC and TIC, was not significantly different from organic carbon content estimated by manometric determination of CO_2 gas resulting from closed tube combustion (paired t-test, $p=0.272$, $n=21$). Hence, in this manuscript, we report and use the organic carbon content estimated by the closed tube combustion method. Salt correction was done for a subset of samples of Stations A, B, and D (1.5, 6.5, 12.5, 16.5, and 20.5 cm layers). However, salt correction (0.02% by weight of dry sediment) did not significantly change SOC content. ^{210}Pb activity was analyzed for Station D samples by measuring the activity of ^{210}Po (Robbins and Edgington, 1975) with an SSB alpha spectrometer (Canberra Inc., PIPS) at the Korea Basic Science Institute; uncertainty was 6.0% RSD.

For carbon isotope analysis, suspended POC samples were fumigated with concentrated HCl and were processed following the same method used for sediment samples, except that silver needles were added before combustion, instead of silver cups. Suspended POC concentration was determined by the amount of CO_2 gas resulting from the closed tube combustion and the volume of filtered water.

3. Results

3.1. POC content and carbon isotope ratios of suspended particles in the surface water

Suspended POC concentration ranged between 0.15 and 0.47 mg C L^{-1} ($n=5$, Fig. 3, Table 1) in February and March 2012. POC concentration in the central polynya (0.45 and 0.47 mg C L^{-1}) was about three times that near the Dotson Ice Shelf (0.15 mg C L^{-1}) and in the sea ice zone (0.17 mg C L^{-1}). Low POC concentration near the Dotson Ice Shelf is consistent with the low chlorophyll-*a* concentration observed by satellite telemetry (La et al., 2015). In general, the chlorophyll-*a* concentration in the upper 10 m of the water column and the suspended POC concentration measured during the cruise showed a positive correlation ($R^2=0.78$, p-value$=0.048$, $n=5$; Yang et al., unpublished data, not shown).

The $\Delta^{14}C$ values of suspended POC varied between −193 and −128‰ with an average of −149 ± 26‰ (Fig. 3, Table 1). The $\Delta^{14}C$ value of suspended POC near the shelf break (−193‰) was significantly lower than $\Delta^{14}C$ values elsewhere (−138 ± 7.3‰, $n=4$). The $\Delta^{14}C$ values of suspended POC were generally similar to that of dissolved inorganic carbon in the surface water (−153‰, 72.40°S, 117.72°W; M. Kim and J. Hwang, unpublished data, 2014). The conventional ^{14}C age (calculated using the equation provided by Stuiver and Polach (1977)) of suspended POC in the surface waters of the Amundsen Shelf was 1200 ± 250 yr, consistent with the standard reservoir effect of ~1300 yr in this region (Berkman and Forman, 1996; Domack et al., 2001). The $\delta^{13}C$ values of suspended POC ranged between −28.4‰ and −24.8‰ with an average of −26.3 ± 1.3‰; the lowest $\delta^{13}C$ value was observed near the Dotson Ice Shelf (Fig. 3).

3.2. Biogeochemical properties of sedimentary organic matter

The SOC content of surface sediments (core-top, 0–1 cm) ranging between 0.5% and 1.1% was greater at the periphery and at the center of the polynya than at other locations (Fig. 4 and

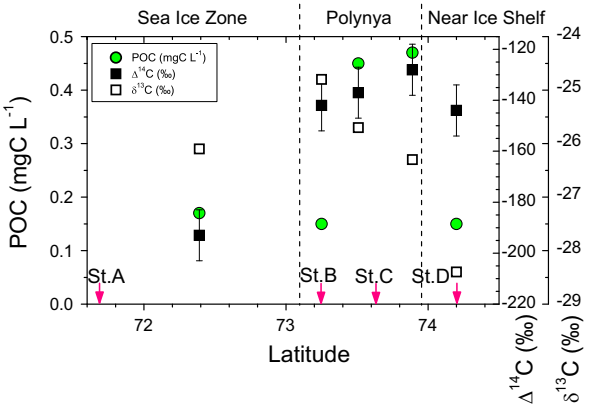

Fig. 3. POC concentration (mg C L^{-1}), $\Delta^{14}C$ (‰), and $\delta^{13}C$ (‰) values of suspended particles collected at ~7 m in surface waters. The latitudes of the sediment sampling sites are also indicated on the *x*-axis.

Table 2). Although located inside the polynya, the SOC content near the Dotson Ice Shelf was significantly lower than at other sites inside the polynya. This difference was also consistently observed down core. The SOC content observed at the periphery is the highest value reported to date for the Amundsen Shelf. From the survey of surface sediments of the Amundsen Sea and the Bellingshausen Sea, excluding the Amundsen Sea polynya region, Hillenbrand et al. (2003) reported SOC content values lower than 0.7%.

The $\Delta^{14}C$ values of the core-top sediment at Stations A, B, C and D were −386‰, −311‰, −349‰, and −418‰, respectively; spatial variation was over 100‰ (Fig. 4). Higher values were observed at the periphery and at the center of the polynya. The lowest value was observed near the Dotson Ice Shelf. SOC content and $\Delta^{14}C$ value were negatively correlated ($R^2=0.8$, p-value$=0.094$, $n=4$; not shown). The average $\Delta^{14}C$ value (-366 ± 50‰, $n=4$) of surface sediments from the Amundsen Shelf was equivalent to an uncorrected ^{14}C age of 3.60 ± 0.59 kyr before present (BP).

Down core SOC content ranged between 0.2% and 1.1% (Fig. 4). Among stations, the vertical variation in SOC content was smaller than the horizontal variation. In general, the SOC content decreased slightly with increasing depth at each station. At Stations B and C, SOC content appears to decrease more monotonically with depth than at Stations A and D. At Station A, SOC content decreased with depth down to 2.5 cm (2–3 cm horizon), then remained constant to a depth of 6.5 cm, below which the values were ~0.3% and no longer showed any discernable trend with increasing depth. At Station D, SOC content increased slightly with depth to 6.5 cm, then decreased to 14.5 cm then remained constant below this depth.

Trends in total carbon (TC) content were virtually identical to SOC trends, because TIC contents were very low, with the exception of Station A. TIC existed in considerable amount only at Station A, where TIC content decreased from 0.7% at 1.5 cm to 0.2% at 12.5 cm, and then approached zero at 16.5 cm and 20.5 cm. TIC contents at Stations B and D were minimal, <0.02%. There are no data on TIC for Station C. Total nitrogen (TN) content ranged between 0.03% and 0.17% (Fig. 4). The average TN content at Stations B and C was about twice that of Stations A and D. The C/N molar ratio at all stations ranged between 6.4 and 13. The C/N molar ratio at Station D (down core average=11) was generally slightly higher (by >2 RSD at most depths) than at the other sites (down core average values at Stations A, B, and C were 9.3, 9.1, and 9.2, respectively).

Down core $\Delta^{14}C$ values of SOC exhibited large vertical and station-to-station variations. $\Delta^{14}C$ values varied more drastically with depth at Stations A and D than at Stations B and C (Fig. 4). At Station A, the $\Delta^{14}C$ value ranged between −386‰ and −860‰. The $\Delta^{14}C$ values in the upper 0–2 cm were identical, but below this layer, the $\Delta^{14}C$ value decreased to 9.5 cm, although the values at 9.5 and 13.5 were again identical. In comparison, the $\Delta^{14}C$ value at Station B decreased almost monotonically from −311‰ at the

Table 1
Concentration and carbon isotope ratios of suspended POC in the surface waters of the Amundsen Sea from February 2012 to March 2012.

Station	Sampling date	Lat. (°S)	Long. (°W)	POC (mg C L^{-1})	$\Delta^{14}C$ (‰)	$\delta^{13}C$ (‰)
6	Mar. 2	72.39	117.72	0.17	−193	−26.1
10	Feb. 12	73.25	114.99	0.15	−142	−24.8
16	Feb. 14	73.51	114.01	0.45	−137	−25.7
71	Feb. 16	73.82	113.07	0.47	−128	−26.3
19	Feb. 16	74.20	112.52	0.15	−144	−28.4

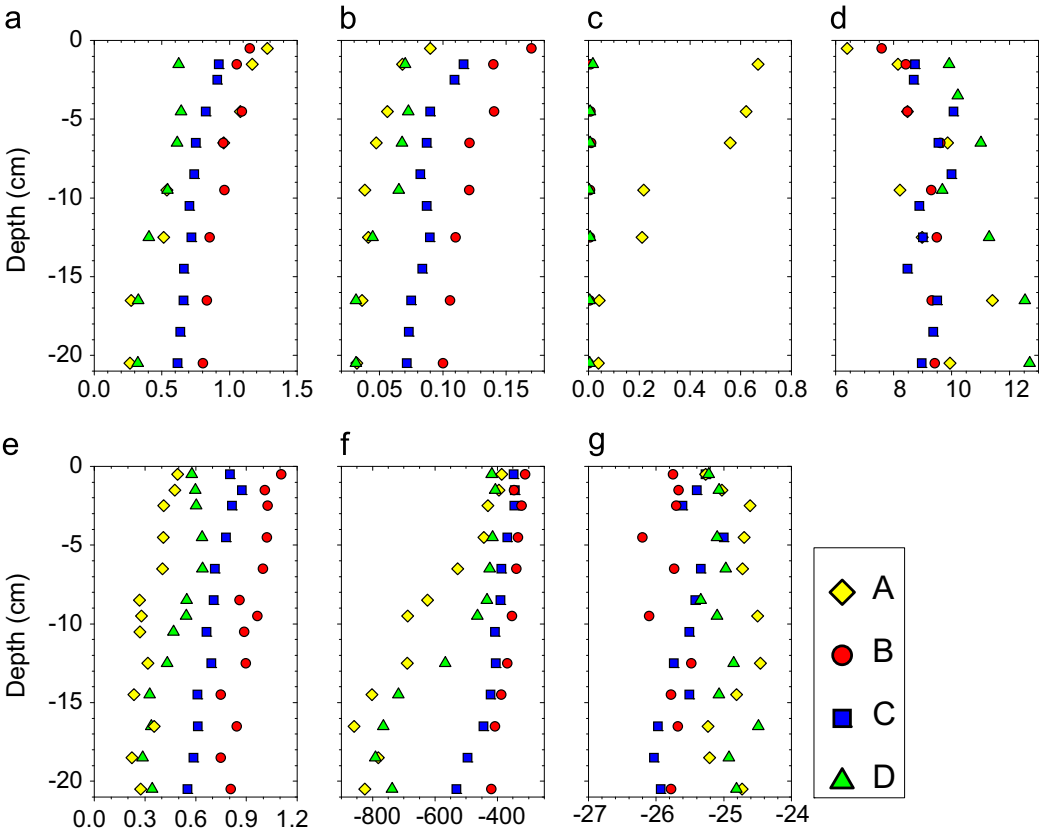

Fig. 4. Vertical distribution of (A) total carbon content, (B) total nitrogen content, (C) total inorganic carbon content, (D) C/N molar ratio, (E) sedimentary organic carbon content, (F) $\Delta^{14}C$ (‰), and (G) $\delta^{13}C$ (‰) in the sediment at four locations: Station A (diamond), Station B (circle), Station C (square), and Station D (triangle).

Table 2
Down core SOC content and carbon isotope ratios of SOC collected at four different locations on the Amundsen Shelf. The reported SOC content was determined manometrically by closed tube combustion.

Depth (cm)	Station A						Station B						Station C						Station D						
	TC (%)	TIC (%)	SOC (%)	TN (%)	C/N molar ratio	$\Delta^{14}C$ (‰)	$\delta^{13}C$ (‰)	TC (%)	TIC (%)	SOC (%)	TN (%)	C/N molar ratio	$\Delta^{14}C$ (‰)	$\delta^{13}C$ (‰)	TC (%)	TIC (%)	SOC (%)	TN (%)	C/N molar ratio	$\Delta^{14}C$ (‰)	$\delta^{13}C$ (‰)	TC (%)	TIC (%)	SOC (%)	TN (%)	C/N molar ratio	$\Delta^{14}C$ (‰)	$\delta^{13}C$ (‰)	^{210}Pb (mBq/g)
0–1	1.3		0.49	0.09	6.4	−386	−25.3	1.2		1.1	0.17	7.6	−311	−25.8			0.80			−349	−25.3			0.58			−418	−25.2	538
1–2	1.2	0.67	0.48	0.07	8.1	−395	−25.0	1.1	0.01	1.0	0.14	8.4	−346	−25.7	0.92		0.87	0.12	8.7	−344	−25.4	0.63	0.02	0.60	0.07	9.9	−407	−25.1	420
2–3			0.41			−430	−24.6			1.0			−322	−25.8	0.91		0.82	0.11	8.7	−346	−25.6			0.60					
4–5	1.1	0.62	0.41	0.06	8.5	−443	−24.7	1.1	0.01	1.0	0.14	8.5	−334	−26.2	0.82		0.78	0.09	10	−368	−25.0	0.64	0.01	0.64	0.07	10	−415	−25.1	330
6–7	1.0	0.56	0.40	0.05	9.9	−527	−24.7	1.0	0.01	1.0	0.12	9.6	−339	−25.7	0.75		0.71	0.09	9.5	−388	−25.3	0.61	0.01	0.64	0.07	11	−424	−25.0	198
8–9			0.27			−624	−25.0			0.85					0.74		0.71	0.08	10	−391	−25.4			0.55			−433	−25.3	
9–10	0.54	0.22	0.27	0.04	8.2	−688	−24.5	1.0	0.01	0.97	0.12	9.3	−353	−26.1								0.54	0.00	0.54	0.07	9.7	−464	−25.1	146
10–11			0.27							0.89					0.71		0.67	0.09	8.9	−408	−25.5			0.47					
12–13	0.51	0.21	0.32	0.04	9.0	−689	−24.5	0.86	0.01	0.90	0.11	9.5	−369	−25.5	0.72		0.69	0.09	9.0	−405	−25.7	0.40	0.01	0.43	0.04	11	−567	−24.9	87
14–15			0.24			−803	−24.8			0.75			−387	−25.8	0.66		0.61	0.08	8.5	−422	−25.5			0.33			−717	−25.1	
16–17	0.27	0.04	0.35	0.04	11	−860	−25.2	0.83	0.00	0.84	0.11	9.3	−408	−25.7	0.66		0.61	0.08	9.5	−445	−26.0	0.33	0.00	0.34	0.03	13	−765	−24.5	
18–19			0.22			−782	−25.2			0.75					0.64		0.59	0.07	9.4	−495	−26.0			0.29			−791	−24.9	
20–21	0.26	0.04	0.27	0.03	9.9	−825	−24.7	0.80	0.00	0.81	0.10	9.4	−420	−25.8	0.62		0.55	0.07	9.0	−531	−25.9	0.32	0.00	0.34	0.03	13	−738	−24.8	

surface to −420‰ at 20.5 cm. The vertical distribution patterns of $\Delta^{14}C$ values at Stations B and C were similar but the values at Station C were systematically lower than those at Station B. At Station D, $\Delta^{14}C$ values were similar from the surface down to 8.5 cm and then decreased with increasing depth down to 16.5 cm. At both Stations A and D, the values at 20.5 cm were higher than those at 16.5 cm. The observed $\Delta^{14}C$ values correspond to uncorrected ^{14}C ages of 3.9–15.7, 2.9–4.3, 3.3–6.0, and 4.1–12.6 kyr BP at Stations A, B, C, and D, respectively (Table 3).

The $\delta^{13}C$ values of surface sediments varied within a narrow range (-25.4 ± 0.2‰, Fig. 4 and Table 2). This is in contrast to the wide variation (± 1.3‰) in $\delta^{13}C$ values observed for suspended POC in surface waters (Fig. 3). The $\delta^{13}C$ values of the surface sediments were within the range of suspended POC values in surface waters. However, no correlation was apparent between the $\delta^{13}C$ values of surface sediments and corresponding suspended POC at each location. At each station, $\delta^{13}C$ values showed a narrow range (within 1‰) of vertical variation in sediments, with no clear trends. In general, $\delta^{13}C$ values increased from Station B to Stations D and A, whereas $\Delta^{14}C$ values decreased from Station B to D to A.

4. Discussion

4.1. Sediment accumulation on the Amundsen Shelf

We can estimate the linear sedimentation rate (LSR) from our detailed ^{14}C age data for the upper 21-cm of sediment. A surface mixed layer of homogeneous ^{14}C age, ranging from 2 to 3 cm in thickness, was apparent at Stations A and C (Fig. 5). The ^{14}C age at 1.5 cm at Station B was distinctly older than the values above and below and hence the surface mixed layer was not well defined. The thickness of the layer of identical ^{14}C age was much greater at Station D than at the other stations. The activity of ^{210}Pb at Station D decreased from about 540 mBq g^{-1} at the top of the core to 90 mBq g^{-1} at 12.5 cm (Fig. 5). If bioturbation did not exist, this ^{210}Pb distribution would suggest a sedimentation rate of 26 cm/kyr, which does not seem plausible in this environment. In such a case, sedimentation of the upper 15 cm layer would take only ~580 yr, which is not consistent with our ^{14}C results. Our ^{14}C results show that the age of SOC has changed from 13 kyr to ~3.9 kyr during that time frame. Therefore, this decrease in ^{210}Pb activity with depth is probably a result of ^{210}Pb penetration due to bioturbation, rather than radioactive decay.

Below the surface mixed layer, ^{14}C age increased linearly with depth down to about 16.5, 20.5, 16.5, and 16.5 cm at Stations A, B, C, and D, respectively (Fig. 5). The LSR was estimated for each of these layers from the slope of the linear regression between the depth and the corresponding ^{14}C age. The LSR determined for the 4.5–16.5, 2.5–20.5, 2.5–16.5, and 9.5–16.5 cm horizons was 1.1 (± 0.3, 95% confidence level, $n=7$), 13 (± 2.2, $n=8$), 12 (± 2.6, $n=8$), and 1.0 (± 0.6, $n=4$) cm/kyr, at Stations A, B, C and D, respectively (Table 4). The LSR at the periphery and at the center of the polynya was one order of magnitude higher than near the shelf break and near the ice shelf. The estimated LSR values represent very different time periods at each station, hence site-to-site comparisons should be made with caution. For example, the LSR is valid for 3.1–4.3 kyr BP at Station B, whereas the LSR is for 4.6–15.7 kyr BP at Station A (both uncorrected ^{14}C ages). The LSR at Station A, near the shelf break, is similar to previously reported values in the western Amundsen Sea rise determined for Marine Isotope Stage I (< 12 kyr BP in calendar age; Hillenbrand et al., 2003).

Unfortunately, at Stations A and D, information on more recent time periods (equivalent to temporal information at Stations B and C) was compromised because of sediment mixing. However, the

Table 3
Radiocarbon ages of sediment horizons. The reservoir effect (1238 yr) was determined from the average ^{14}C age of the suspended POC collected from the surface waters of the Amundsen Sea.

Depth (cm)	Station A				Station B				Station C				Station D			
	$\Delta^{14}C$ (‰)	^{14}C age (kyr)			$\Delta^{14}C$ (‰)	^{14}C age (kyr)			$\Delta^{14}C$ (‰)	^{14}C age (kyr)			$\Delta^{14}C$ (‰)	^{14}C age (kyr)		
		Uncorr.	Corr. for reservoir effect	Corr. for core-top age		Uncorr.	Corr. for reservoir effect	Corr. for core-top age		Uncorr.	Corr. for reservoir effect	Corr. for core-top age		Uncorr.	Corr. for reservoir effect	Corr. for core-top age
0–1	−386	3.86	2.62	0	−311	2.93	1.69	0	−349	3.38	2.14	0	−418	4.29	3.05	0
1–2	−395	3.98	2.74	0.12	−346	3.36	2.12	0.43	−344	3.32	2.08	0	−407	4.13	2.89	0
2–3	−430	4.45	3.21	0.59	−322	3.06	1.82	0.13	−346	3.35	2.11	0				
4–5	−443	4.64	3.40	0.78	−334	3.20	1.96	0.27	−368	3.63	2.39	0.25	−415	4.24	3.00	0
6–7	−527	5.95	4.71	2.09	−339	3.27	2.03	0.34	−388	3.88	2.64	0.50	−424	4.37	3.13	0.08
8–9	−624	7.79	6.55	3.93					−391	3.92	2.68	0.54	−433	4.50	3.26	0.21
9–10	−688	9.30	8.06	5.44	−353	3.44	2.20	0.51					−464	4.95	3.71	0.66
10–11									−408	4.15	2.91	0.77				
12–13	−689	9.32	8.08	5.46	−369	3.63	2.39	0.70	−405	4.12	2.88	0.74	−567	6.66	5.42	2.37
14–15	−803	13.0	11.8	9.14	−387	3.87	2.63	0.94	−422	4.34	3.10	0.96	−717	10.1	8.81	5.76
16–17	−860	15.7	14.5	11.8	−408	4.15	2.91	1.22	−445	4.67	3.43	1.29	−765	11.6	10.3	7.26
18–19	−782	12.2	10.9	8.29					−495	5.43	4.19	2.05	−791	12.6	11.3	8.26
20–21	−825	14.0	12.7	10.1	−420	4.31	3.07	1.38	−531	6.02	4.78	2.64	−738	10.7	9.46	6.41

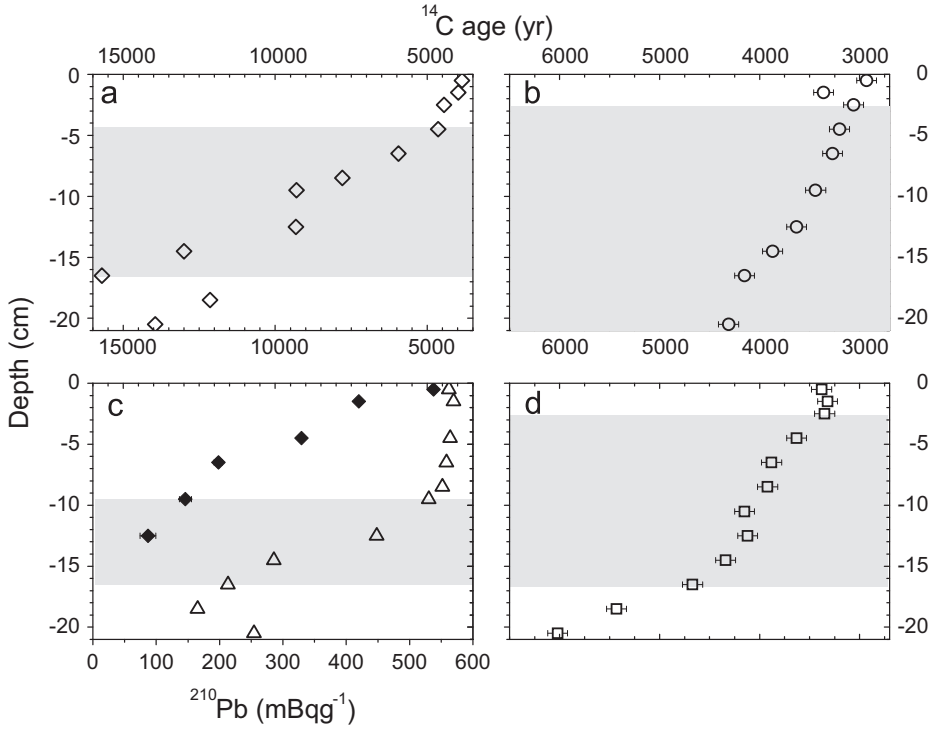

Fig. 5. Vertical distribution of uncorrected ^{14}C ages at four stations. Shaded layers denote the sediment horizons for which linear sedimentation rates were determined. Error bars for ^{14}C ages at Stations A and D are smaller than the symbols. At station D, ^{210}Pb activity is also shown (closed diamonds). Note that the *x*-axis scales of the left and right panels are different.

average ^{14}C age of SOC in the surface mixed layer provides a constraint for the lower limit of the LSR. The lowest possible LSR is obtained when the POC currently being deposited derives from fresh production alone. The lower limits of the LSR thus estimated are 1.5 and 0.8 cm/kyr at Stations A and D, respectively. Because there was likely an additional supply of aged POC to these sites, the actual LSRs are expected to be higher than these estimates.

At Station C, in the central polynya, a sudden down core change in LSR from 12 cm/kyr to 3 cm/kyr was observed at about 16 cm, corresponding to 4.7 kyr BP in uncorrected ^{14}C age (about 1.3 kyr BP in core-top age-corrected ^{14}C age). A similar change was not observed at Station B, which may be because the temporal coverage of the examined sediment layer was too short. This change in LSR likely indicates a sudden change in the depositional environment. Potential causes may include changes in biological production associated with polynya development and/or enhancement of sediment supply from a lateral transport of allochthonous particles caused by changes in water circulation patterns. Alternatively, the occasional penetration of bioturbation down to 16 cm may be responsible for the observed shift in the LSR. Without other supporting information, the cause of this change cannot be determined.

Inversion of ^{14}C age with depth was observed at both Stations A and D but at different times. The oldest samples correspond to 15.7 and 12.6 kyr BP in uncorrected ^{14}C age at Stations A and D, respectively (or, when corrected by subtraction of the core-top

Table 4
Properties of the core-top sediments (0–1 cm) and linear sedimentation rates (LSR) and sedimentary organic carbon accumulation rates.

	Stations			
	A	B	C	D
$\Delta^{14}C$ (‰)	−386	−311	−349	−418
$\delta^{13}C$ (‰)	−25.3	−25.8	−25.3	−25.2
SOC (%)	0.49	1.1	0.80	0.58
LSR in cm/kyr	1.1 ± 0.3	13 ± 2	12 ± 3	1.0 ± 0.6
(depths in cm)	(4.5–16.5)	(2.5–20.5)	(2.5–16.5)	(9.5–16.5)
SOC accumulation rate (g C m^{-2} yr^{-1})	0.05	1.2	0.9	0.06

age, 11.8 and 8.3 kyr BP, respectively). Based on reconstruction of past ice sheet retreats (Kirshner et al., 2012; Larter et al., 2014) the grounding line passed Station A relatively early, before 13.8 kyr BP. In comparison, Station D was under the ice shelf until at least 10.6 kyr BP. Deglacial sediments are often characterized by a sharp increase in ^{14}C age with depth, caused by a contamination of fossil organic matter (referred to as a 'dog leg'; e.g., Smith et al., 2011). The oldest layers at Stations A and D and the inversion in ^{14}C age immediately below these layers may be related to the retreat of grounded ice and/or the ice shelf. However, the inversion was not accompanied by any drastic change in SOC content. Therefore, the cause of the inversion is not clear.

The minimal TIC content observed in sediments at Stations B and D is consistent with previous studies (e.g., Hillenbrand et al., 2003; Hauck et al., 2012). The low TIC content likely reflects the low abundance of calcifiers in the Antarctic (Smith et al., 2011). The TIC content of sinking particles in the sea ice zone was < 2% during the whole trap deployment period (in 2011) at 400 m (72.40°S, 117.72°W, 530 m bottom depth) (Kim et al., 2015). Much smaller values, < 0.2%, were observed during the austral summer (Kim et al., 2015). Carbonate compensation depth in the Amundsen Sea was estimated at about 4000 m (Hillenbrand et al., 2003) and is not likely to cause the low sedimentary TIC content. Only Station A exhibited considerable TIC content: ~0.7% (equivalent to ~6% as $CaCO_3$) in the surface sediment (Fig. 4). TIC content started to increase up core from < 0.05% at 16.5 cm, where the ^{14}C age (corrected by core-top sediment age) was about 11.8 kyr BP. This timing matches the suggested onset of $CaCO_3$ increase in this region, about 12.0 kyr BP (Hillenbrand et al., 2003).

4.2. Characteristics of organic carbon accumulation on the Amundsen Shelf

The SOC accumulation rate in the sediment was calculated based on average water content, average SOC content, the LSR, and an estimated sediment density of 2.7 ± 0.2 g/cm^3 (based on the clay mineralogy on the Amundsen Shelf, Ehrmann et al., 2011). For example, at Station A, the SOC accumulation rate = dry sediment content (48%) × density (2.7 g/cm^3) × SOC content (0.32%) × LSR (1.1 cm/kyr) = 0.05 g C m^{-2} yr^{-1}. The estimated SOC accumulation rates were 0.05, 1.2, 0.9, and 0.06 g C m^{-2} yr^{-1} at Stations A, B, C, and D, respectively, with an uncertainty of ~ ± 30% (~60% at Station D; Table 4). The distinctly higher SOC accumulation rates (~20 times greater than at the other sites) observed at the periphery and at the center of the polynya were consistent with the high primary productivity associated with the polynya. The SOC content, core-top $\Delta^{14}C$ values, and SOC accumulation rates at the periphery and at the center of the polynya were consistently different from the other sites. These observations imply that biological production is likely a major controlling factor for SOC accumulation on the Amundsen Shelf. Similar trends and values were observed in the Ross Sea (DeMaster et al., 1996). The SOC accumulation rate was 0.3 ± 0.2 g C m^{-2} yr^{-1} in the southwestern part of the Ross Sea (two exceptionally high values near the Granite Harbor were excluded), whereas it was 0.04 ± 0.01 g C m^{-2} yr^{-1} in the northeastern part of the Ross Sea (DeMaster et al., 1996).

Within the polynya, the SOC accumulation rates at the periphery and at the center were not statistically different, in contrast to the spatial distribution of primary productivity determined in situ during the cruise in late December 2010–January 2011 (Lee et al., 2012). Primary production around Station B was much higher than that at Stations A and D, but lower than that at Station C (Lee et al., 2012). Satellite based observation in the polynya consistently shows lower chlorophyll-*a* concentrations in the periphery compared to the center of the polynya (Arrigo et al., 2012; La et al., 2015). Further research is needed to understand the reason for this discrepancy between the SOC accumulation rate and primary production in the overlying water column.

In addition to fresh biological production, aged POC from sediment resuspension and/or glacial melt may constitute another important source of POC. Accumulation of the shallow mixed layer (~3 cm) with relatively high LSRs (~12 cm/kyr) at Stations B and C would take only about 230–250 yr. In a simplistic model where the only source of POC to the sediment was fresh production in the overlying surface water, the age of the mixed layer is estimated to be older than the source POC by only about 160 yr. We used a model similar to that in Griffith et al. (2010) with the exception that the SOC was one component with the degradation rate of 0.002 yr^{-1} (a value that yields observed, ~0.8% SOC content) and that a fixed value of ^{14}C content of source POC was used. The estimated ^{14}C age therefore is distinctly younger than the measured ^{14}C age of the surface mixed layer at Stations B and C (3.12–3.35 kyr). This result implies that allochthonous, aged POC is supplied to these sites, and/or particulate organic matter undergoes resuspension/settling cycles many times before final sedimentation. The annual average current speed was ~6.8 cm/s with a maximum of 27 cm/s at 430 m (73.28°S, 114.95°W; 370 m above the seafloor) inside the polynya and ~4.9 cm/s with a maximum of 18 cm/s at 409 m depth (72.40 °S, 117.72 °W; 130 m above the seafloor) in the sea ice zone (Ha et al., unpublished data). This current may be strong enough to facilitate sediment resuspension and lateral transport of particles (Lampitt, 1985; Lampitt et al., 2000). Aged POC from the ice shelf, transported by the melt water plume, may constitute an additional source (Jenkins et al., 2010). The majority of sinking POC intercepted at 400 m in the sea ice zone was freshly produced POC, based on $\Delta^{14}C$ results (flux-weighted $\Delta^{14}C$ value = −173‰; Kim et al., 2015). This implies that the lateral supply of aged POC and/or the resuspension/deposition cycle of POC occur mainly below the trap depth, near the seafloor. Stations B and C are not likely to be the depocenters, although they are located on the slope of the Dotson trough, because the dominant deep flow is along the trough (Ha et al., 2014). Furthermore, the higher SOC content at these sites argues against the possibility that most of the sediment was supplied from other locations where the SOC content is lower.

4.3. Shelf-wide organic carbon accumulation

The uncorrected ^{14}C ages of the core-top sediment (ranging between 2.9 and 4.3 kyr BP) are considerably younger than reported

for the same region by Smith et al., 2011 (3.9–7.3 kyr BP, obtained from the acid-insoluble organic fraction of surface sediments). Although there are discrepancies of up to 2.1 kyr between the ages of bulk SOC and the acid-insoluble fraction, the general trend is consistent: younger values at around 73.1 °S (Station BC429 in Smith et al., 2011) and older values immediately north of the Dotson Ice Shelf (Stations BC416 and BC420 in Smith et al., 2011). There is a positive relationship between the ^{14}C ages of the bulk SOC of the core-top sediments in this study and the acid-insoluble fraction of the adjacent surface sediments (Smith et al., 2011) in the study region (^{14}C age of bulk SOC $= 0.519 \times$ ^{14}C age of acid-insoluble fraction $+ 1046$, $R^2 = 0.95$, p-value $= 0.025$, Fig. 6A). The ^{14}C age of the acid-insoluble fraction of core-top sediment at BC435; the average value of BC410, BC423, BC429, and 267-2; the average value of BC421, BC426, and 265-3; and the average value of BC416 and BC420 in Smith et al. (2011) correspond to Stations A, B, C, and D, respectively, and were used for the linear regression (Fig. 6A). This discrepancy in ^{14}C ages likely reflects the heterogeneity in the ^{14}C ages of each component of the SOC in this region: bulk organic matter (containing both freshly produced, labile POC and a potentially refractory, pre-aged acid-insoluble organic fraction) is likely to be younger (^{14}C ages) than the acid-insoluble organic fraction (Wang et al., 1998; Hwang et al., 2005). However, it should be noted that this relationship is the result of supplies from various POC sources and early-diagenetic processes and the coefficients of the linear relationship may not be used for extrapolation.

A general feature of the ^{14}C age distribution of bulk SOC in surface sediments can be gleaned from a more comprehensive ^{14}C age dataset reported by Smith et al. (2011) (Fig. 7). Inside the Amundsen Sea, polynyas are characterized by comparatively young ^{14}C ages (3233 ± 333 on average, $n = 12$). An exception is the region immediately north of the Dotson Ice Shelf, where the oldest values were observed (4433 ± 176 on average, $n = 4$). ^{14}C ages outside the polynya lie between these two values (3729 ± 89 on average, $n = 4$). ^{14}C age of the surface sediment is expected to have a negative correlation with SOC accumulation rate if the main source of POC to sediment is contemporaneous production. Our data also exhibited a weak negative relationship between the two parameters (Fig. 6B, $R^2 = 0.88$, p-value $= 0.06$). Therefore, a general feature of the SOC accumulation on the Amundsen Shelf can be gleaned from the spatial distribution of the ^{14}C age of SOC in surface sediments.

If we extrapolate our SOC accumulation results to the western Amundsen Sea embayment (between 110°W and 120°W) and divide the embayment into two regions (a polynya-associated, high SOC accumulation region and the remaining ice-ridden, low SOC accumulation region), the total SOC accumulation rate is estimated to be approximately 3×10^{10} g C yr^{-1}. The mean SOC accumulation rate at Stations B and C, 1.0 g C m^{-2}yr^{-1}, was used for the Amundsen Sea polynya that has the summer opening area of 27,000 km^2 (Arrigo et al., 2012), whereas the value at Station A, 0.05 g C m^{-2} yr^{-1}, was used for the rest of the region ($86{,}000 - 27{,}000 = 59{,}000$ km^2). The uncertainty for this estimate is likely larger than ~30% (for SOC accumulation alone) because the spatial variability in the ^{14}C age of the surface sediment was not properly determined and considered (Figs. 6B and 7). Our results suggest that the Amundsen Sea polynya is responsible for ~90% of the total SOC burial, although it occupies only 30% of the western Amundsen Shelf (areally) between 110°W and 120°W. This is a simplistic estimate that does not account for smaller scale spatial variability. Further research based on more data will be needed to refine this preliminary value.

5. Summary

As part of a larger study to characterize the biological pump operating currently and in the recent past in the Amundsen Sea, we examined organic carbon accumulation in western Amundsen Shelf sediments, based mainly on radiocarbon analysis of bulk SOC. We determined SOC content and carbon isotope ratios in the upper 21-cm of sediment at four locations with different summertime sea ice cover, bottom depth, and distance from the coast and the ice shelf.

Depending on location, the examined sediment layers corresponded to widely different time periods, ranging from 2.9 to 15.7 kyr BP (in uncorrected ^{14}C age). The LSRs at the stations inside the Amundsen Sea polynya, about 12 cm/kyr during the time period of 3.1–4.7 kyr BP (uncorrected ^{14}C age), were higher than those near the shelf break (1.1 cm/kyr during the time period of 4.6–15.7 kyr BP) and near the ice shelf (1.0 cm/kyr during the time period of 5.0–11.6 kyr BP). SOC accumulation rates at polynya-associated sites were ~20 times that at other sites because of higher SOC contents and LSRs inside the polynya. The higher SOC accumulation rate appears to be correlated with the high primary production in the polynya. Although located within the polynya, the site near the Dotson Ice Shelf exhibited an order of magnitude lower SOC accumulation rate compared to the other sites associated with the polynya; this lower SOC accumulation rate, is consistent with the primary productivity previously determined in situ in surface waters (Lee et al., 2012).

Station C, at the center of the polynya, exhibited a sudden change in LSR at around 4.7 kyr BP (uncorrected ^{14}C age) corresponding to 1.3 kyr BP if the ^{14}C age of the core-top sediment is subtracted. This sudden change may be caused by changes in the physical environment at the surface, such as polynya development and/or changes in deep currents, enhancing the lateral supply of allochthonous particles. Further examination of other properties, such as phytoplankton composition and primary productivity recorded in sediments, is warranted.

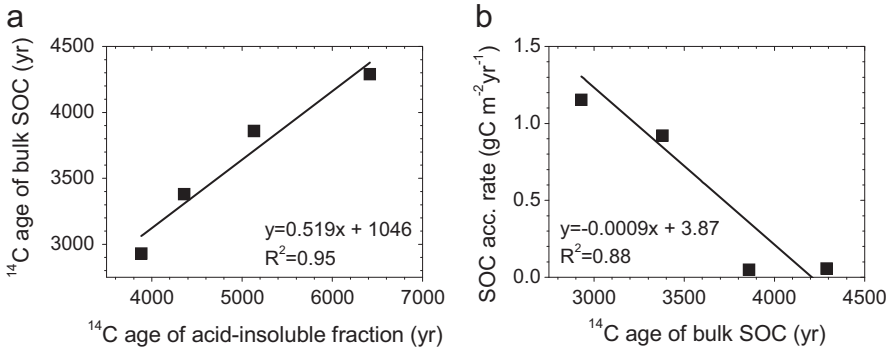

Fig. 6. (A) The correlation between the ^{14}C age of bulk SOC (this study) and that of the acid-insoluble fraction of sedimentary organic matter at adjacent sites reported by Smith et al. (2011) and (B) the correlation between SOC accumulation rates and ^{14}C ages of bulk SOC of core-top sediments.

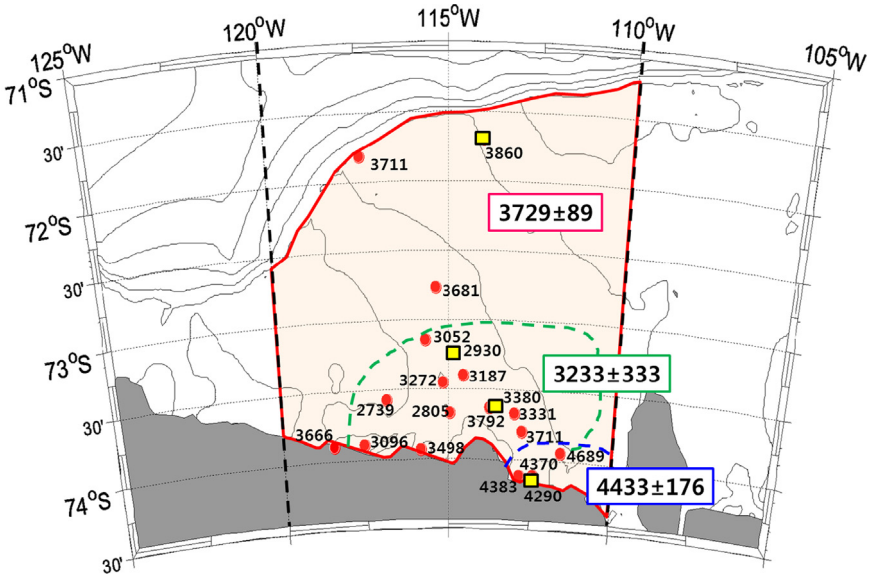

Fig. 7. ^{14}C ages of bulk SOC measured (squares; this study) and estimated from those of the acid-insoluble SOC fraction (circles; Smith et al., 2011) on the western Amundsen Shelf. The dashed lines divide the sea ice zone outside the polynya, the polynya, and the region proximal to the Dotson Ice Shelf.

Based on the distinct SOC accumulation rates for the two regions (the polynya-associated region and the remaining sea-ice covered region), SOC accumulation on the western Amundsen Sea embayment between 110°W and 120°W is estimated to be about 3×10^{10} g C yr^{-1} (the uncertainty of this preliminary estimate is likely to be larger than ~30%). Thus, the Amundsen Sea polynya is responsible for ~90% of the SOC burial, although it occupies only 30% of the western Amundsen Shelf area between 110°W and 120°W.

Acknowledgments

We thank the captain and the crew of the IBRV *Araon* for help at sea; Heung Soo Moon for help with sediment sampling; NOSAMS WHOI for carbon isotope analyses; the Korea Basic Science Institute for the ^{210}Pb measurements and the TC and TN analyses; and Haryun Kim, Dhong Il Lim, Do Hyeon Jeong, and Bu Yeong Lee at KIOST for the TC, TIC, and TN analyses. JH was partly supported by Research Resettlement Fund for the new faculty of Seoul National University. This research was supported by the Korea Polar Research Institute (PP 15020).

References

Arrigo, K.R., van Dijken, G.L., 2003. Phytoplankton dynamics within 37 Antarctic coastal polynya systems. J. Geophys. Res. 108, 3271.
Arrigo, K.R., Lowry, K.E., van Dijken, G.L., 2012. Annual changes in sea ice and phytoplankton in polynyas of the Amundsen Sea, Antarctica. Deep-Sea Res. II 71–76, 5–15.
Becquevort, S., Smith Jr., W.,O., 2001. Aggregation, sedimentation and biodegradability of phytoplankton-derived material during spring in the Ross Sea, Antarctica. Deep-Sea Res. II 48, 4155–4178.
Berkman, P.A., Forman, S.L., 1996. Pre-bomb radiocarbon and the reservoir correction for calcareous marine species in the Southern Ocean. Geophys. Res. Lett. 23, 363–366.
Broecker, W.S., Olson, E.A., 1959. Lamont radiocarbon measurements VI. Am. J. Sci. 1, 111–132.
DeMaster, D.J., Ragueneau, O., Nitteouer, C.A., 1996. Preservation efficiencies and accumulation rates for biogenic silica and organic C, N, and P in high-latitude sediments: The Ross Sea. J. Geophys. Res. 101, 18501–18518.
Domack, E., Leventer, A., Dunbar, R., Taylor, F., Brachfeld, S., Sjunneskog, C., 2001. Chronology of the Palmer Deep site, Antarctic Peninsula: a Holocene palaeoenvironmental reference for the circum-Antarctic. Holocene 11, 1–9.
Ducklow, H.W., Erickson, M., Lee, S., Lowry, K., Post, A., Sherrell, R., Stammerjohn, S., Wilson, S., Yager, P., 2015. Particle flux on the continental shelf in the Amundsen Sea Polynya and Western Antarctic Peninsula. Elementa 3, 000046.
Ehrmann, W., Hillenbrand, C.D., Smith, J.A., Graham, A.G., Kuhn, G., Larter, R.D., 2011. Provenance changes between recent and glacial-time sediments in the Amundsen Sea embayment, West Antarctica: clay mineral assemblage evidence. Antarct. Sci. 23, 471–486.
Fragoso, G.M., Smith Jr., W.O., 2012. Influence of hydrography on phytoplankton distribution in the Amundsen and Ross Seas, Antarctica. J. Mar. Syst. 89, 19–29.
Griffith, D.R., Martin, W.R., Eglinton, T.I., 2010. The radiocarbon age of organic carbon in marine surface sediments. Geochim. Cosmochim. Acta 74, 6788–6800.
Ha, H.K., Wåhlin, A., Kim, T., Lee, S., Lee, J., Lee, H., Hong, C., Arneborg, L., Björk, G., Kalén, O., 2014. Circulation and modification of warm deep water on the central Amundsen Shelf. J. Phys. Oceanogr. 44, 1493–1501.
Hauck, J., Gerdes, D., Hillenbrand, C.D., Hoppema, M., Kuhn, G., Nehrke, G., Völker, C., Wolf-Gladrow, D.A., 2012. Distribution and mineralogy of carbonate sediments on Antarctic shelves. J. Mar. Syst. 90, 77–87.
Hedges, J.I., Stern, J.H., 1984. Carbon and nitrogen determinations of carbonate-containing solids. Limnol. Oceanogr. 29, 657–663.
Hillenbrand, C.D., Grobe, H., Diekmann, B., Kuhn, G., Fütterer, D.K., 2003. Distribution of clay minerals and proxies for productivity in surface sediments of the Bellingshausen and Amundsen seas (West Antarctica)–Relation to modern environmental conditions. Mar. Geol. 193, 253–271.
Hwang, J., Druffel, E.R., Komada, T., 2005. Transport of organic carbon from the California coast to the slope region: A study of $\Delta^{14}C$ and $\delta^{13}C$ signatures of organic compound classes. Glob. Biogeochem. Cycles 19, GB2018, doi:2010.1029/2004GB002422.
Jenkins, A., Dutrieux, P., Jacobs, S.S., McPhail, S.D., Perrett, J.R., Webb, A.T., White, D., 2010. Observations beneath Pine Island Glacier in West Antarctica and implications for its retreat. Nat. Geosci. 3, 468–472.
Kim, M., Hwang, J., Kim, H.J., Kim, D., Yang, E.J., Ducklow, H.W., La, H.S., Lee, S.H., Park, J., Lee, S., 2015. Sinking particle flux in the sea ice zone of the Amundsen Shelf, Antarctica. Deep-Sea Res. I 101, 110–117. http://dx.doi.org/10.1016/j.dsr.2015.04.002.
Kirshner, A.E., Anderson, J.B., Jakobsson, M., O'Regan, M., Majewski, W., Nitsche, F.O., 2012. Post-LGM deglaciation in Pine Island Bay, West Antarctica. Quat. Sci. Rev. 38, 11–26.
Komada, T., Anderson, M.R., Dorfmeier, C.L., 2008. Carbonate removal from coastal sediments for the determination of organic carbon and its isotopic signatures, $\delta^{13}C$ and $\Delta^{14}C$: comparison of fumigation and direct acidification by hydrochloric acid. Limnol. Oceanogr. Methods 6, 254–262.
La, H.S., Lee, H., Fielding, S., Kang, D., Ha, H.K., Atkinson, A., Park, J., Siegel, V., Lee, S., Shin, H.C., 2015. High density of ice krill (*Euphausia crystallorophias*) in the Amundsen sea coastal polynya, Antarctica. Deep-Sea Res. I 95, 75–84.
Lampitt, R., 1985. Evidence for the seasonal deposition of detritus to the deep-sea floor and its subsequent resuspension. Deep-Sea Res. I 32, 885–897.
Lampitt, R., Newton, P., Jickells, T., Thomson, J., King, P., 2000. Near-bottom particle flux in the abyssal northeast Atlantic. Deep-Sea Res. II 47, 2051–2071.
Larter, R.D., Anderson, J.B., Graham, A.G., Gohl, K., Hillenbrand, C.D., Jakobsson, M., Johnson, J.S., Kuhn, G., Nitsche, F.O., Smith, J.A., 2014. Reconstruction of changes in the Amundsen Sea and Bellingshausen Sea sector of the West Antarctic Ice Sheet since the Last Glacial Maximum. Quat. Sci. Rev. 100, 55–86.
Lee, S.H., Kim, B.K., Yun, M.S., Joo, H., Yang, E.J., Kim, Y.N., Shin, H.C., Lee, S., 2012. Spatial distribution of phytoplankton productivity in the Amundsen Sea, Antarctica. Polar Biol. 35, 1721–1733.
McNichol, A., Osborne, E., Gagnon, A., Fry, B., Jones, G., 1994. TIC, TOC, DIC, DOC, PIC, POC – unique aspects in the preparation of oceanographic samples for ^{14}C-AMS 92, 162–165Nucl. Instrum. Meth. B 92, 162–165.

Pritchard, H.D., Arthern, R.J., Vaughan, D.G., Edwards, L.A., 2009. Extensive dynamic thinning on the margins of the Greenland and Antarctic ice sheets. Nature 461, 971–975.

Rignot, E., Bamber, J.L., Van Den Broeke, M.R., Davis, C., Li, Y., Van De Berg, W.J., Van Meijgaard, E., 2008. Recent Antarctic ice mass loss from radar interferometry and regional climate modelling. Nat. Geosci. 1, 106–110.

Robbins, J.A., Edgington, D.N., 1975. Determination of recent sedimentation rates in Lake Michigan using Pb-210 and Cs-137. Geochim. Cosmochim. Acta 39, 285–304.

Smith, J.A., Hillenbrand, C.D., Kuhn, G., Larter, R.D., Graham, A.G., Ehrmann, W., Moreton, S.G., Forwick, M., 2011. Deglacial history of the West Antarctic Ice Sheet in the western Amundsen Sea embayment. Quat. Sci. Rev. 30, 488–505.

Stammerjohn, S., Massom, R., Rind, D., Martinson, D., 2012. Regions of rapid sea ice change: An inter-hemispheric seasonal comparison. Geophys. Res. Lett. 39, L0501.

Stuiver, M., Polach, H.A., 1977. Discussion; reporting of ^{14}C data. Radiocarbon 19, 355–363.

Volk, T., Hoffert, M.I., 1985. Ocean carbon pumps: analysis of relative strengths and efficiencies in ocean-driven atmospheric CO_2 changes. In: Sundquist, E.T., Broecker, W.S. (Eds.), The Carbon Cycle and Atmospheric CO_2: Natural Variations Archean to Present. Geophys. Monogr. Ser. vol. 32, pp. 99–110.

Walker, D.P., Brandon, M.A., Jenkins, A., Allen, J.T., Dowdeswell, J.A., Evans, J., 2007. Oceanic heat transport onto the Amundsen Sea shelf through a submarine glacial trough. Geophys. Res. Lett. 34, 1–4.

Wang, X.-C., Druffel, E.R., Griffin, S., Lee, C., Kashgarian, M., 1998. Radiocarbon studies of organic compound classes in plankton and sediment of the northeastern Pacific Ocean. Geochim. Cosmochim. Acta 62, 1365–1378.

Zielinski, U., Gersonde, R., 1997. Diatom distribution in Southern Ocean surface sediments (Atlantic sector): implications for paleoenvironmental reconstructions. Palaeogeogr. Palaeoclimatol. Palaeoecol. 129, 213–250.